RNA-Seq and Mass-Spectrometry-Based Lipidomics Reveal Extensive Changes of Glycerollipid Pathways in Brown Adipose Tissue in Response to Cold

Marcher, Ann-Britt; Loft, Anne; Nielsen, Ronni; Vihervaara, Terhi; Madsen, Jesper Grud Skat; Sysi-Aho, Marko; Ekroos, Kim; Mandrup, Susanne

Published in:
Cell Reports

DOI:
10.1016/j.celrep.2015.10.069

Publication date:
2015

Document Version
Publisher's PDF, also known as Version of record

Cell Reports

Resource

RNA-Seq and Mass-Spectrometry-Based Lipidomics Reveal Extensive Changes of Glycerolipid Pathways in Brown Adipose Tissue in Response to Cold

Graphical Abstract

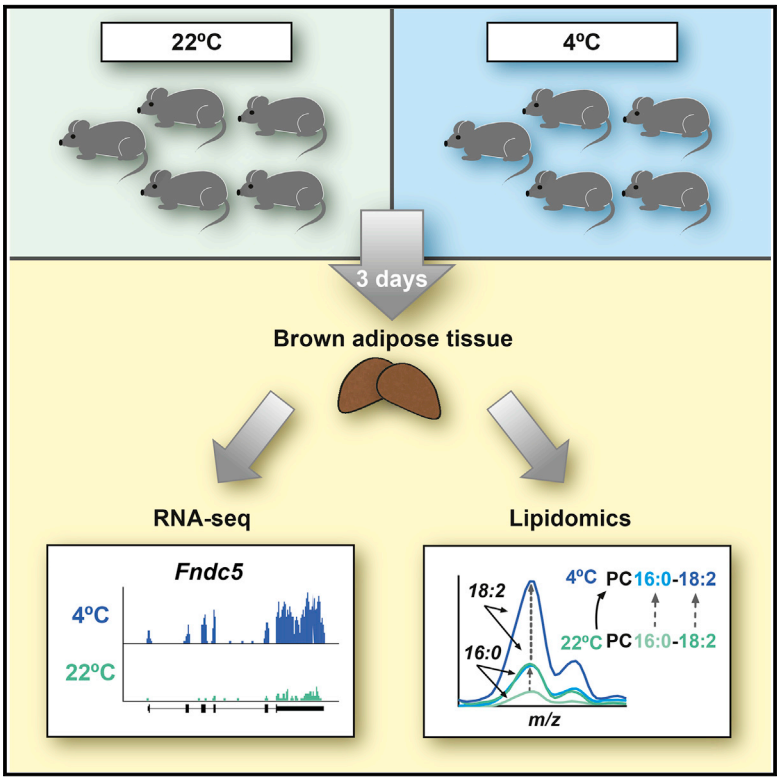

Authors

Ann-Britt Marcher, Anne Loft, Ronni Nielsen, ..., Marko Sysi-Aho, Kim Ekroos, Susanne Mandrup

Correspondence

s.mandrup@bmb.sdu.dk

In Brief

Using RNA-seq and mass-spectrometry-based lipidomics, Marcher et al. demonstrate that the early adaptation of brown adipose tissue to cold exposure entails induction of gene pathways involved in triacylglycerol and phospholipid metabolism and a highly selective remodeling of the glycerolipid content in the tissue.

Highlights

- This study integrates transcriptome/lipidome analysis of BAT in cold-exposed mice
- Cold exposure induces glycerolipid gene programs
- Long-chain and odd-numbered acyl chains in TAGs are increased in response to cold
- Glycerophospholipid species are differentially remodeled in response to cold

Accession Numbers

GSE70437

Marcher et al., 2015, Cell Reports *13*, 2000–2013
December 1, 2015
http://dx.doi.org/10.1016/j.celrep.2015.10.069

CellPress

OPEN ACCESS
CellPress

Cell Reports
Resource

RNA-Seq and Mass-Spectrometry-Based Lipidomics Reveal Extensive Changes of Glycerolipid Pathways in Brown Adipose Tissue in Response to Cold

Ann-Britt Marcher,[1,4] Anne Loft,[1,4] Ronni Nielsen,[1] Terhi Vihervaara,[3] Jesper Grud Skat Madsen,[1,2] Marko Sysi-Aho,[3] Kim Ekroos,[3] and Susanne Mandrup[1,*]

[1]Department of Biochemistry and Molecular Biology, University of Southern Denmark, 5230 Odense M, Denmark
[2]Novo Nordisk Foundation Center of Basic Metabolic Research, University of Copenhagen, 2200 Copenhagen, Denmark
[3]Zora Biosciences Oy, Biologinkuja 1, 02150 Espoo, Finland
[4]Co-first author
*Correspondence: s.mandrup@bmb.sdu.dk
http://dx.doi.org/10.1016/j.celrep.2015.10.069

SUMMARY

Cold exposure greatly alters brown adipose tissue (BAT) gene expression and metabolism to increase thermogenic capacity. Here, we used RNA sequencing and mass-spectrometry-based lipidomics to provide a comprehensive resource describing the molecular signature of cold adaptation at the level of the transcriptome and lipidome. We show that short-term (3-day) cold exposure leads to a robust increase in expression of several brown adipocyte genes related to thermogenesis as well as the gene encoding the hormone irisin. However, pathway analysis shows that the most significantly induced genes are those involved in glycerophospholipid synthesis and fatty acid elongation. This is accompanied by significant changes in the acyl chain composition of triacylglycerols (TAGs) as well as subspecies-selective changes of acyl chains in glycerophospholipids. These results indicate that cold adaptation of BAT is associated with significant and highly species-selective remodeling of both TAGs and glycerophospholipids.

INTRODUCTION

Brown adipose tissue (BAT) plays an important role in defending body temperature in rodents during cold exposure by inducing non-shivering thermogenesis. This process occurs mainly in BAT and relies on the large number of mitochondria that are partially uncoupled because of the expression of uncoupling protein 1 (UCP1) (Cannon and Nedergaard, 2004). Another hallmark of this type of adipose tissue is that it is highly innervated and vascularized. The vascularization ensures a supply of oxygen and metabolic substrates as well as the distribution of heat generated by the tissue, whereas the sympathetic innervation controls the activity of the tissue through β-adrenergic receptors on brown adipocytes (Cannon and Nedergaard, 2004). Cold exposure increases β-adrenergic activation of brown adipocytes, thereby activating lipolysis of the triacylglycerol (TAG) stores and liberating fatty acids, the major fuel substrates for thermogenesis. In addition, BAT takes up large amounts of glucose and lipids from the circulation that are used for thermogenesis (Bartelt et al., 2011; Labbe et al., 2015). The ability to dissipate energy and to clear circulating lipids and glucose (Bartelt et al., 2011; Labbe et al., 2015) makes BAT an attractive potential therapeutic target for the prevention of obesity.

Acute cold exposure stimulates the activity of BAT and the expression of the thermogenic gene program, including UCP1. Sustained cold exposure (weeks) leads to increased thermogenic potential of BAT in mice through mitochondrial biogenesis, increased vascularization (Xue et al., 2009), and increased tissue mass (Cinti, 2005). In addition, short-term cold exposure of mice has been shown recently, by digital gene expression (DGE) profiling, to induce the activation of gene programs related to glucose metabolism in BAT (Hao et al., 2015). Furthermore, the expression of a broad range of genes involved in lipid metabolic reactions has been shown to change upon cold exposure, including ELOVL fatty acid elongase 3 (*Elovl3*), lipoprotein lipase (*Lpl*), acyl-coenzyme A (CoA) synthetase long-chain (*Acsl*) family members 1/3/4/5, 1-acylglycerol-3-phosphate O-acyltransferase (*Agpat*) 1/2/3/5/6, and diacylglycerol O-acyltransferase (*Dgat*) 1/2 (Hao et al., 2015; Rosell et al., 2014; Shore et al., 2013; Yu et al., 2002). However, it remains poorly understood how the BAT lipidome is altered in response to short-term cold exposure.

In this study, we applied RNA sequencing (RNA-seq) combined with mass-spectrometry-based lipidomics to determine the effect of short-term (3-day) cold exposure on gene expression and the lipidome of interscapular BAT (iBAT) of C57BL/6J mice. We show that cold exposure leads to marked changes in the expression of genes involved in lipid metabolism, especially those involved in glycerophospholipid metabolism and fatty acid elongation, and we find that these changes are accompanied by a previously undescribed complexity in glycerophospholipid remodeling. These comprehensive datasets constitute a valuable resource that will be useful in future targeted investigations of the cold-induced changes in BAT lipid composition and gene expression.

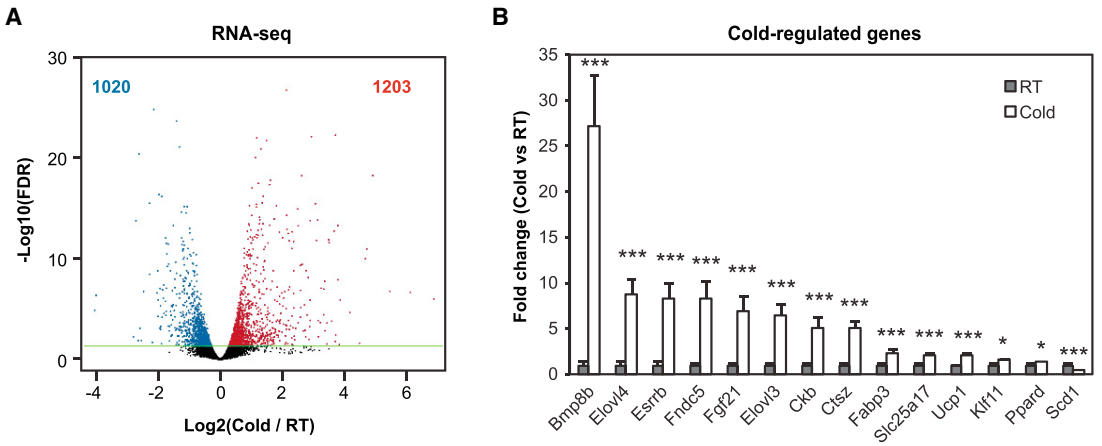

C

KEGG pathways (p<0.01) associated with top 250 genes induced by cold

TermID	Term	P-value	Genes in Term	Target Genes in Term	Gene Symbols
mmu00564	**Glycerophospholipid metabolism**	8.5E-06	91	9	**Pgs1,Ptdss2,Lpgat1,Gpd1,Pla2g12a,Agpat1,Ppap2a,Agpat3,Phospho1**
mmu_M00415	**Fatty acid biosynthesis, elongation, endoplasmic reticulum**	3.8E-04	10	3	**Ptplb,Elovl4,Elovl3**
mmu00561	**Glycerolipid metabolism**	1.4E-03	55	5	**Gyk,Mgll,Ppap2a,Agpat3,Agpat1**
mmu_M00089	**Triacylglycerol biosynthesis**	1.6E-03	16	3	**Ppap2a,Agpat1,Agpat3**
mmu00565	**Ether lipid metabolism**	3.3E-03	41	4	**Pla2g7,Ppap2a,Pafah2,Pla2g12a**
mmu00062	**Fatty acid elongation**	5.4E-03	24	3	**Ptplb,Elovl4,Elovl3**

KEGG pathways (p<0.01) associated with top 250 genes repressed by cold

TermID	Term	P-value	Genes in Term	Target Genes in Term	Gene Symbols
mmu00480	**Glutathione metabolism**	7.6E-09	54	10	**Gstt2,Mgst3,Gstm1,Gpx8,Gpx4,Gclc,Gstt1,Gpx3,Gpx1,Gstm2**
mmu00982	**Drug metabolism - cytochrome P450**	7.3E-06	66	8	**Gstt2,Mgst3,Maob,Gstm1,Gstt1,Adh1,Aox1,Gstm2**
mmu00980	**Metabolism of xenobiotics by cytochrome P450**	4.5E-04	64	6	**Gstm1,Gstt2,Gstt1,Adh1,Mgst3,Gstm2**
mmu00630	**Glyoxylate and dicarboxylate metabolism**	6.4E-04	26	4	**Pccb,Hyi,Gcsh,Grhpr**
mmu00280	**Valine, leucine and isoleucine degradation**	1.1E-03	51	5	**Aldh2,Aldh6a1,Pccb,Hmgcs2,Aox1**
mmu00640	**Propanoate metabolism**	1.4E-03	32	4	**Aldh2,Aldh6a1,Pccb,Acss2**
mmu00260	**Glycine, serine and threonine metabolism**	3.3E-03	40	4	**Aoc3,Gcsh,Grhpr,Maob**
mmu00350	**Tyrosine metabolism**	4.0E-03	42	4	**Adh1,Aoc3,Aox1,Maob**
mmu00620	**Pyruvate metabolism**	4.3E-03	43	4	**Aldh2,Pcx,Acss2,Grhpr**

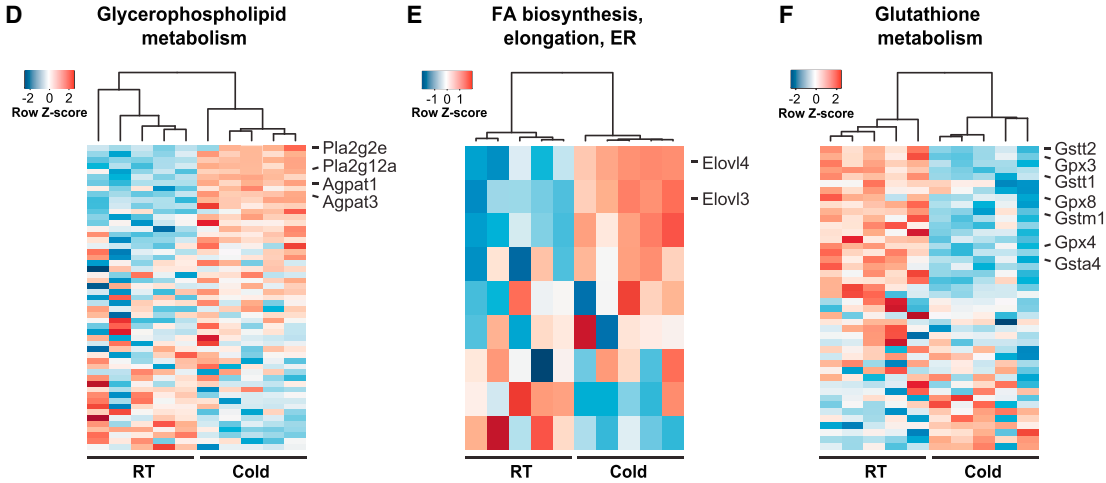

Figure 1. Short-Term Exposure to Cold Induces Gene Programs Involved in Lipid Metabolism

Mice were kept at room temperature or exposed to cold (4°C) for 3 days. iBAT was isolated, and RNA was purified for RNA-seq. Differential mRNA expression between cold-treated and control samples was determined with EdgeR.

(A) Log2 fold changes in exons of RefSeq gene bodies in cold-treated versus control mice and the corresponding significance values displayed as −log10(FDR). The green line indicates the cutoff value for differential expression (FDR < 0.05). In total, 1,203 and 1,020 genes were identified that had induced (red) or repressed (blue) expression levels by cold exposure. RT, room temperature. Only genes with -log(FDR) <30 are displayed.

(legend continued on next page)

RESULTS

Cold Exposure Dramatically Changes the Expression of Genes Involved in Glycerolipid Metabolism and Fatty Acid Elongation

To map the transcriptional changes in iBAT in response to cold, we exposed male C57BL/6J mice to either room temperature (22°C) or cold (4°C) for 3 days and subsequently isolated RNA for RNA-seq. We chose room temperature (22°C) as the housing condition for our control mice because this constitutes the temperature for most physiological studies. It is known that this temperature leads to a mild cold challenge in mice (Golozoubova et al., 2004), and it is therefore important to note that iBAT in our control group is slightly activated; i.e., we are not comparing inactive with active iBAT. Rather, we are comparing "normal," slightly activated iBAT with more activated iBAT.

Using a significance level of FDR < 0.05, we found a total of 2,223 differentially expressed genes, of which 1,203 and 1,020 genes show increased and reduced expression, respectively, by 3-day cold exposure (Figure 1A). Notably, several genes reported previously as having increased expression upon cold exposure, such as the genes encoding uncoupling protein 1 (*Ucp1*) (Grefhorst et al., 2015; Waldén et al., 2012), fibroblast growth factor 21 (*Fgf21*) (Chartoumpekis et al., 2011; Grefhorst et al., 2015; Hondares et al., 2011), bone morphogenetic protein 8b (*Bmp8b*) (Grefhorst et al., 2015; Rosell et al., 2014; Whittle et al., 2012), and creatine kinase, brain (*Ckb*) (Hao et al., 2015), display significantly higher expression levels in BAT after cold exposure (Figure 1B). Interestingly, we also detected a markedly increased expression of Kruppel-like factor 11 (*Klf11*), which we recently identified as a browning factor in human adipose-derived stem cells (Loft et al., 2015), as well as fibronectin type III domain containing 5 (*Fndc5*), which encodes the prohormone FNDC5 (irisin), which has been reported to promote browning of white adipose tissue (WAT) (Boström et al., 2012; Figure 1B).

Functional enrichment analyses of the top 250 genes with the most pronounced cold-induced expression using Kyoto Encyclopedia of Genes and Genomes (KEGG) pathways (Kanehisa and Goto, 2000; Kanehisa et al., 2014) revealed a significant enrichment of metabolic pathways, including glycero- and glycerophospholipid metabolism (Figure 1D), fatty acid biosynthesis and elongation (Figure 1E), as well as TAG biosynthesis (Figure 1C). Genes related to these pathways include phospholipase A2 (*Pla2*) group IIE/XIIA (Figure 1D), *Agpat 1* and *3* (Figure 1D), and *Elovl 3* and *4* (Figure 1E). The most highly enriched pathway for downregulated genes is glutathione metabolism (Figures 1C and 1F), which includes several genes encoding glutathione peroxidases (*Gpx 3, 4, and 8*) and glutathione S-transferases (*Gsta 4, Gstm 1, and Gstt 1 and 2*) (Figure 1F). Because increased activity of GPx and GST has been observed in murine iBAT in response to cold treatment (Petrović et al., 2006), the decrease at their mRNA levels might reflect an inhibitory feedback circuit. Taken together, we found extensive changes in the transcriptome of murine iBAT in response to 3 days of cold challenge (4°C) compared with normal housing conditions at 22°C. These changes included a marked increase in the expression of genes involved in glycerolipid metabolism.

Cold-Induced Changes in the Transcriptome Are Highly Dependent on Experimental Conditions

The effect of cold on global gene expression in murine iBAT has been investigated in a few other studies using microarray or DGE profiling (Figure 2A). These studies were performed under different conditions, but, in all cases, mice were exposed to cold (4–8°C) for a maximum of 10 days. A comprehensive list of genes with information about fold changes and significance levels obtained by cold exposure in these different studies is presented in Table S1. We first took an unbiased approach and compared the changes in gene expression for a group of genes consisting of the top 250 cold-induced genes in each of the different studies. Hierarchal clustering of datasets based on the log2 fold change in gene expression for this group of genes revealed that the two DGE datasets (Hao et al., 2015) (2 and 4 days of cold treatment) cluster closely together, whereas our study and the 10-day cold exposure study (Rosell et al., 2014) are more distantly associated with this cluster (Figure 2B). The two studies with acute cold exposure for 24 hr (Shore et al., 2013) and 4 hr (Plaisier et al., 2012)) are even more distantly related (Figure 2B). This pattern is also observed when clustering is performed on log2 fold changes for all analyzed genes (Figure S1A). Notably, except for the two DGE datasets (Hao et al., 2015), there is only a very moderate correlation between the cold-induced changes observed in the different studies, indicating that the different experimental conditions, including housing temperature for control mice, gender of the mice, length of study, and detection methods lead to marked differences in expression of the cold-regulated gene programs (Figures 2C, S1B, and S1C). As an example of this, only two studies (Hao et al., 2015; Rosell et al., 2014) detected significant overall changes in the expression of genes related to glucose metabolism, whereas our study and two others (Plaisier et al., 2012; Shore et al., 2013) failed to detect significant changes in this pathway (Figure 1C; Table S2). A possible reason for this is that the control mice in the studies by Hao et al. (2015) and Rosell et al. (2014) were maintained at thermoneutrality, whereas control mice in the other studies were housed at 22°C.

(B) Relative expression levels of selected cold-regulated genes from the RNA-seq dataset for cold-treated and control mice. Data are presented as means + SEM (n = 5). Significance levels: *FDR < 0.05, ***FDR < 0.001.

(C) Genes that were among the top 250 induced and the top 250 repressed in response to cold were subjected to functional enrichment analyses using HOMER. Significantly enriched (p < 0.01) metabolic pathways extracted from the KEGG database are shown for genes with cold-induced (top) and cold-repressed (bottom) expression. Only pathways with ten or more genes are displayed.

(D–F) Scaled expression values for five control (RT) and five cold-treated (4°C) mice for all identified genes in the most significantly enriched metabolic KEGG pathways for genes with cold-induced expression (glycerophospholipid metabolism, D; fatty acid [FA] biosynthesis, elongation, and ER, E) and genes with cold-repressed expression (glutathione metabolism, F). The log2 expression values for each sample were centered and scaled in the row direction (row *Z* score). Hierarchical clustering of samples was based on Pearson's correlation coefficient. The genes mentioned in the text are highlighted on the heatmaps.

A

Studies of global cold-induced changes in gene expression in brown adipose tissue

Study	Strain	Gender	Age	n	Temp.	Days	Techn.
Marcher et al., 2015	C57BL/6J	M	8w	5	22 → 4°C	3	Seq
Hao et al., 2015	C57BL/6J	M	8w	3-4	30 → 4°C	2+4	DGE
Rosell et al., 2014	Sv129	F	10w	4	22 → 28°C vs 22 → 6°C	10	Array
Shore et al., 2013	C57BL/6	F	-	4	22 → 8°C	1	Array
Plaisier et al., 2012	C57BL/6J	M	6-8w	2	22 → 4°C	4h	Array

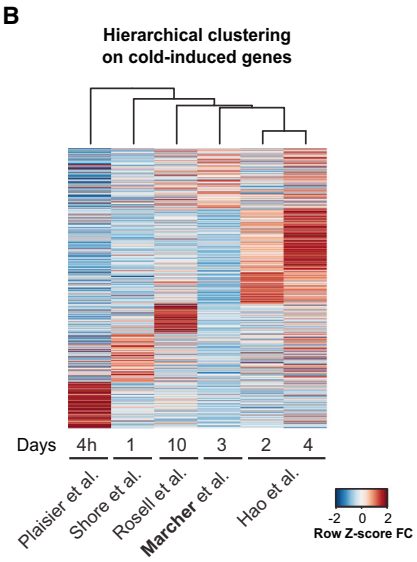

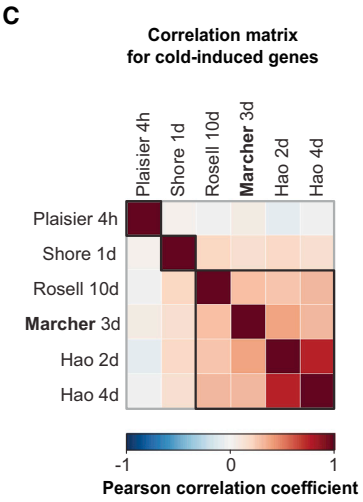

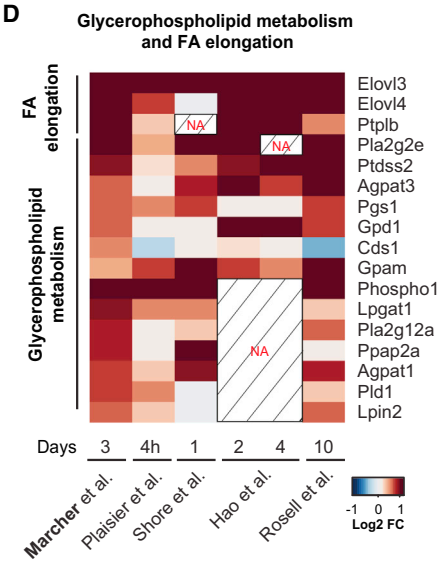

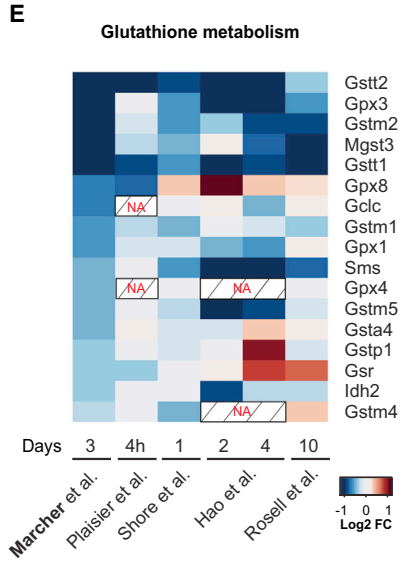

Figure 2. Comparison of Cold-Induced Gene Programs

Publically available microarray and DGE profiling datasets as well as our RNA-seq data from mice exposed to cold and control mice at either room temperature or thermoneutrality were analyzed as described in the Experimental Procedures.

(A) Experimental information for the included studies. Temp, temperature; Techn, technique; M, male; F, female; w, weeks.

(B) Log2 fold changes for the top 250 genes with induced expression from each study in cold-treated versus control mice were extracted, centered, and scaled in the row direction (row *Z* score). Only genes with reported log2 changes in all studies were included in this heatmap. Hierarchical clustering of samples was based on Pearson's correlation coefficient. FC, fold change.

(C) Correlation matrix for all included studies based on Pearson's correlation coefficient for the subset of genes with cold-induced expression described in (B). The matrix was reordered based on hierarchical clustering, with the black squares representing three distinct clusters. h, hours; d, day(s).

(D and E) Log2 fold changes between cold-treated and control mice in all included studies for genes with significantly (FDR < 0.05) cold-induced expression identified in our study within the glycerophospholipid metabolism and fatty acid elongation (D) and genes with cold-repressed expression within the glutathione metabolism (E) KEGG pathways. NA, data not available.

See also Figure S1 and Table S2.

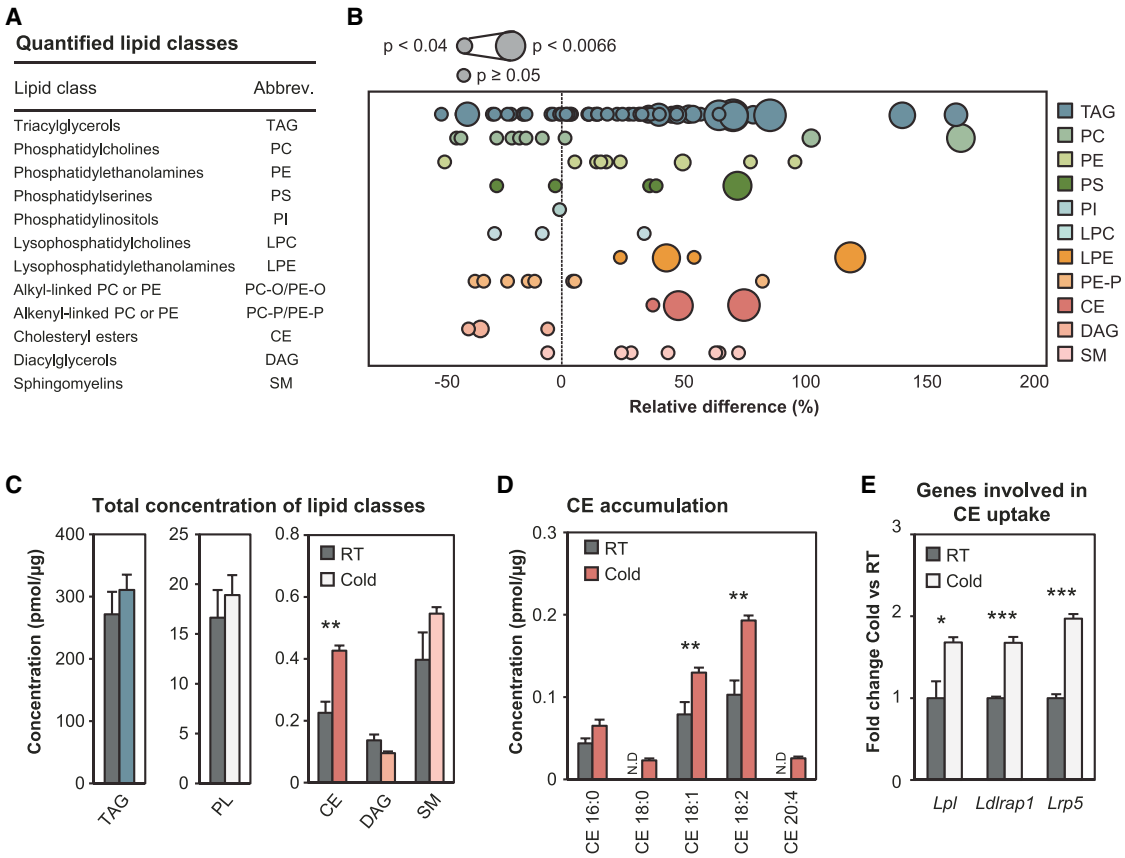

Figure 3. Changes in Overall Lipid Composition of iBAT upon Short-Term Cold Exposure

Lipidomics analysis of iBAT isolated from mice kept at room temperature (22°C) or exposed to cold (4°C) for 3 days. Lipids were extracted and analyzed as described in the Experimental Procedures.

(A) Quantified lipid classes and their abbreviations used throughout the paper.

(B) The relative percentage difference in concentration of all quantified lipid species between cold-treated and control mice. Species that were only detected in one of the groups are omitted from this plot. Each dot represents a lipid species, and the dot size indicates significance. The different lipid classes are color-coded and are used consistently throughout the paper. n = 3–5 for both groups.

(C) The concentration of the quantified lipid classes in iBAT of cold-treated and control mice. PL is the sum of the concentrations of the quantified phospholipids. Data are presented as means + SEM; n = 5 for both groups. Significance level: **p < 0.01.

(D) The concentration of the quantified CE species in iBAT of cold-treated and control mice. Data are presented as means + SEM; n = 5 for both groups. Significance level: **p < 0.01. N.D., not detected.

(E) Relative expression levels of selected genes from the RNA-seq data that are involved in cholesterol uptake for cold-treated and control mice. Data are presented as means + SEM (n = 5). Significance levels: *FDR < 0.05, ***FDR < 0.001.

See also Tables S3 and S4.

None of the previous studies reported that cold exposure leads to an overall induction of the metabolic pathway terms glycerophospholipid and fatty acid elongation. However, a comparison of the cold-induced changes in gene expression from the included studies (Figure 2A) revealed that expression of many of the genes from these metabolic pathways tend to be induced by cold exposure in the other datasets (Figure 2D). For most genes, these changes do not reach statistical significance, most likely because of a low statistical power (Table S2). Similarly, the significantly downregulated expression of genes within the glutathione metabolism pathway also tends to occur in the other studies (Figure 2E).

Taken together, the cold-induced changes in gene expression in mouse iBAT differ markedly between the different studies, most likely as a result of different experimental conditions, detection methods, and degrees of statistical power. Our study demonstrates a major induction of the gene programs involved in glycerophospholipid metabolism and fatty acid elongation, and most other studies show a trend toward increased expression of these genes. These findings suggest that cold exposure induces considerable alterations in lipid metabolic pathways.

Overall Concentrations of Major Lipid Classes Are Only Affected Marginally by Cold Exposure

We next applied mass-spectrometry-based lipidomics to determine how short-term cold exposure affects the composition and distribution of TAG and glycerophospholipid species and acyl chains in iBAT. Quantification of the lipid classes in Figure 3A

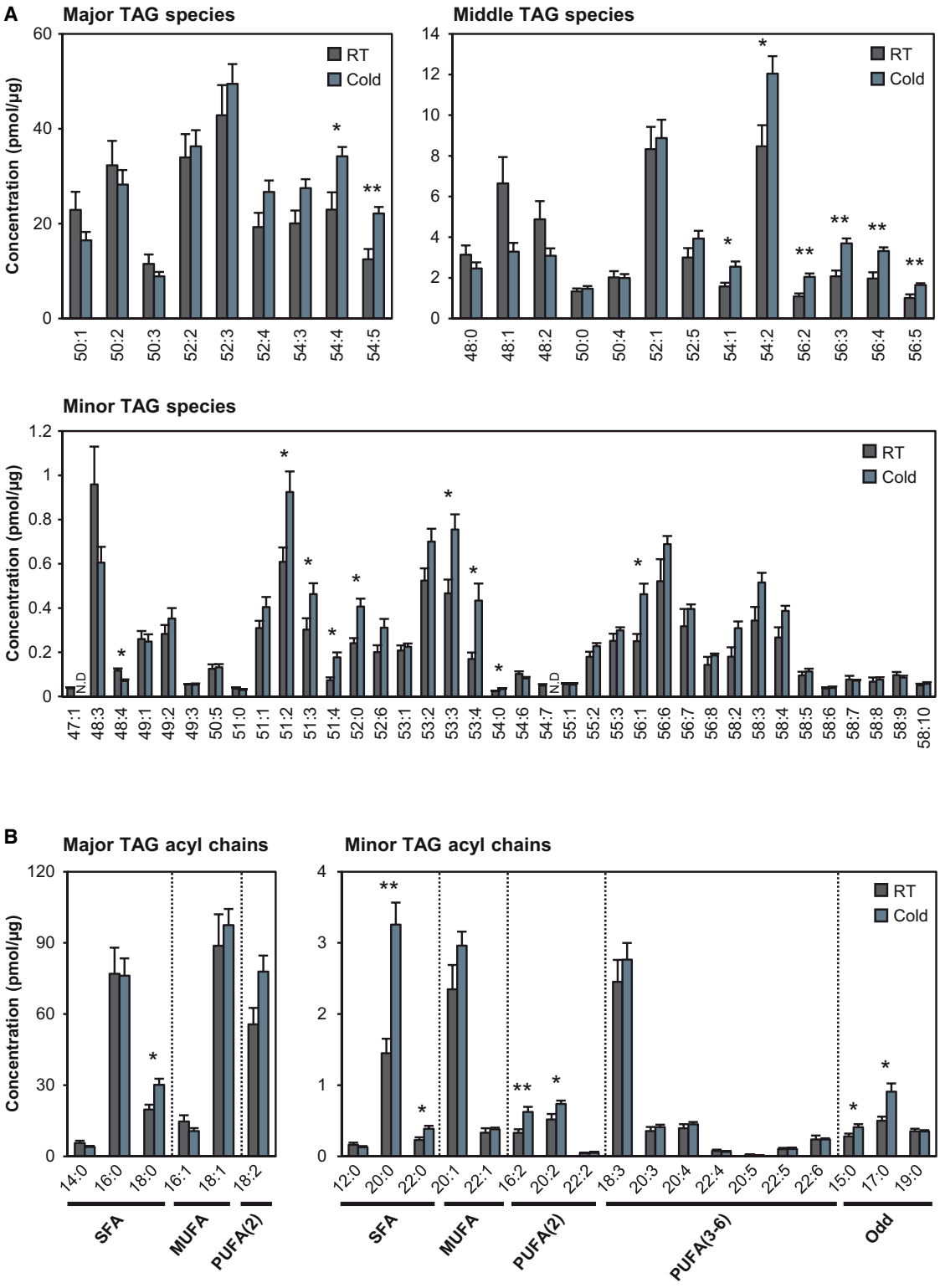

Figure 4. Cold-Mediated Changes in TAG Composition and Fatty Acyl Levels in iBAT

TAG lipidomics of iBAT isolated from mice kept at room temperature (22°C) or exposed to cold (4°C) for 3 days. Lipids were extracted and analyzed as described in the Experimental Procedures.

(legend continued on next page)

revealed significant cold-induced changes in the abundance of lipid species in most of the analyzed lipid classes (Figure 3B). The overall abundance of TAGs and glycerophospholipids, which are the most and secondmost abundant lipid classes in iBAT, respectively, are not affected by cold exposure (Figure 3C). In contrast, we detected an approximately 60% increase in the concentration of cholesteryl esters (CEs) in response to cold (Figure 3C). Further analysis showed that this increase is caused by increased levels of CEs containing C18:1 and C18:2 acyl chains (Figure 3D). It has been reported previously that cold exposure accelerates the uptake of lipoprotein remnants in iBAT (Bartelt et al., 2011), and, because C18:1 and C18:2 are the most abundant fatty acids in the feed (Table S3), our data indicate that an increased bulk flow of fatty acids and lipids into iBAT may drive the increase in CEs. In line with this, the expression of several genes encoding enzymes involved in cholesterol and lipoprotein uptake and turnover, e.g., *Lpl*, low-density lipoprotein receptor adaptor protein 1 (*Ldlrap1*), and low-density lipoprotein receptor-related protein 5 (*Lrp5*) (Fujino et al., 2003; Harada-Shiba et al., 2004), are upregulated by cold exposure in our study (Figure 3E).

Cold Exposure Changes the Length of Fatty Acyl Chains Associated with TAG

Analysis of TAG species revealed no change in the total concentration of TAG (Figure 3C). However, there are numerous dramatic changes in the composition of the species (Figure 4A; Table S4) as well as in the total concentration of individual fatty acyl chains associated with TAG (Figure 4B; Table S4). Because of the analytical challenge of quantifying molecular TAGs, not all species could be distinguished from each other and are therefore reported as brutto lipids (i.e., TAG52:3 contains a mixture of TAG(16:0-18:1-18:2) and TAG(16:1-18:1-18:1)). Interestingly, TAG species containing odd-numbered fatty acyl chains, i.e., C15:0 and C17:0, show the most dramatic relative increase in iBAT upon cold exposure (e.g., TAG51:4, TAG53:4), although these are minor TAG species (Figure 4A). In keeping with this, we detected markedly increased levels of the saturated odd-numbered acyl chains, especially C17:0 but also C15:0, in the TAG pool of iBAT from the cold-exposed mice compared with mice housed at room temperature (Figure 4B). Because the chow diet used for this study does not contain odd-numbered fatty acids (Table S3), the accumulation of odd-numbered acyl chains in TAG must be generated by metabolism, possibly as a result of peroxisomal α-oxidation of long-chain fatty acids that are subsequently esterified into TAG. Alternatively, the increased abundance of the odd-numbered fatty acyls may be a result of increased use of propionyl-CoA instead of acetyl-CoA for fatty acid synthesis (Roncari and Mack, 1976; Seyama et al., 1981; Smith, 1994).

Very-long-chain fatty acyls ($\geq$20 carbons) constitute minor fatty acyls in TAG (Figure 4B). Interestingly, however, cold exposure led to a pronounced accumulation of numerous TAG species containing long- and very-long-chain saturated fatty acyls; e.g., TAG54:2, TAG 56:2, and TAG 56:4 (Figure 4A). Consistent with these changes in TAG species, we detected a robust increase in the levels of the C18:0, C20:0, and C22:0 acyl chains in TAG (Figure 4B), which is in accordance with a previous report (Westerberg et al., 2006). The increase in levels of long to very long fatty acids may have resulted from increased fatty acid elongase activity, because cold exposure greatly induces expression of *Elovl3*, the gene encoding the main enzyme involved in elongation of saturated and monounsaturated C18-C22 fatty acid substrates (Guillou et al., 2010; Figure 1B).

In summary, cold exposure leads to increased expression of genes encoding enzymes involved in TAG synthesis and fatty acid elongation, and markedly changes the composition of fatty acyls associated with TAG species in BAT (Figure 5).

The Glycerophospholipid Pathway Is Stimulated by Short-Term Cold Exposure

Because glycerophospholipid metabolism was the most significant cold-induced gene pathway in our study (Figure 1C), we analyzed how the composition of the different glycerophospholipid classes may be affected by cold exposure. Although cold exposure did not alter the overall abundance of the different glycerophospholipid classes in iBAT (except for the minor lysophosphatidylethanolamine [LPE]; Figure 6A), cold decreased the level of numerous minor glycerophospholipid species to below the limit of detection (Figure 6C). When analyzing the total pool of fatty acyl chains associated with glycerophospholipids, we detected a marked reduction in C16:1 (Figure 6D). A similar reduction in C16:1 in the total pool of glycerophospholipids has been reported previously in iBAT of mice exposed to cold (Ocloo et al., 2007; Ricquier et al., 1979). However, we found that the reduced level of C16:1 upon cold exposure was specifically caused by a marked reduction (to below detection level) in the level of phosphatidylethanolamine (PE), phosphatidylcholine (PC), and lysophosphatidylcholine (LPC) species that contained C16:1 acyl chains (Figure 6C). This decrease may be the result of an almost 50% reduction in expression of stearoyl-CoA desaturase 1 (*Scd1*) (Figures 1B and 5), encoding the main enzyme responsible for desaturation of palmitic and stearic acid. Furthermore, we detected a trend toward a general increase in C18:0 in glycerophospholipids upon cold exposure, although this did not reach statistical significance ($p = 0.0576$) because of a large variation between the animals. However, when quantified for the individual glycerophospholipid subclasses, C18:0 was highly increased in both PC and PE (Figure 6D), and C18:2 was increased in both the PE and phosphatidylserine (PS) subclasses. Therefore, we found that the cold-induced changes in glycerophospholipid acyl chain composition were associated with distinct subclasses. Further analysis of the

(A) The concentration of the quantified TAG species in iBAT from cold-treated (n = 5) and control (n = 3–5) mice. Data are presented as means + SEM. The TAG species are divided into major, middle, and minor species based on abundance. Significance levels: *$p < 0.05$, **$p < 0.01$.
(B) The concentration of individual acyl chains associated with TAG in iBAT from cold-treated (n = 5) and control (n = 4–5) mice. Data are presented as means + SEM. Fatty acyls are divided into major and minor species based on abundance. The fatty acyl chains are sorted by degree of saturation, and the odd-numbered fatty acyls are grouped. Significance levels: *$p < 0.05$, **$p < 0.01$. SAF, saturated fatty acyls; MUFA, monounsaturated fatty acyls; PUFA, polyunsaturated fatty acyls containing two or three to six double bonds; Odd, odd-numbered fatty acyls.

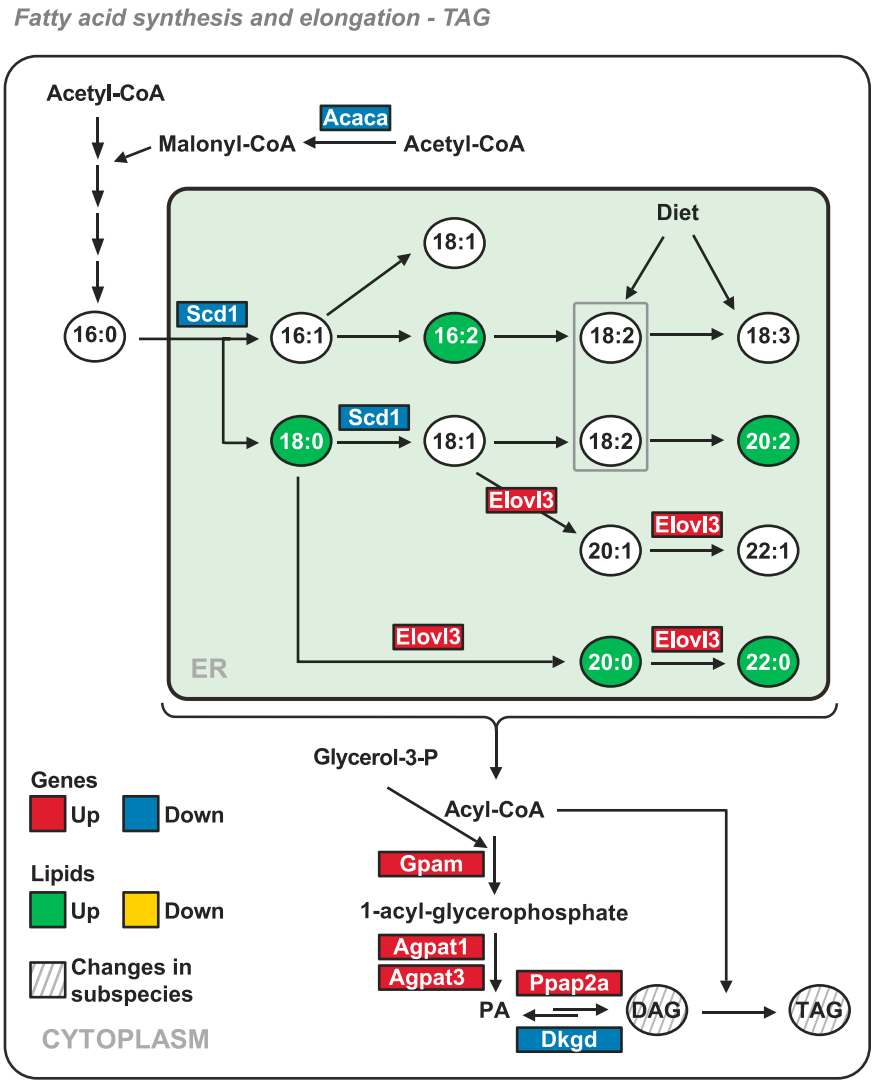

Figure 5. The Fatty Acid Elongation and TAG Biosynthesis Pathways Are Induced in iBAT upon Cold Exposure

Selected fatty acid elongation and glycerophospholipid metabolic reactions from KEGG, with indications of quantified lipid classes and acyl chains (circles) and genes (rectangles) significantly regulated in iBAT by short-term cold exposure. Colors indicate increased (red) or decreased (blue) expression levels of genes (encoding proteins that catalyze the indicated conversions) upon cold exposure or increased (green), decreased (yellow), and unchanged (white) levels of the total concentration of the lipid classes. Lipid classes in which individual subspecies are altered by cold exposure are hatched. PA, phosphatidic acid; *Acaca*, acetyl-coenzyme A carboxylase 1; *Gpam*, glycerol-3-phosphate acyltransferase, mitochondrial; *Ppap2a*, phosphatidic acid phosphatase type 2A; *Dkgd*, diacylglycerol kinase delta. For other abbreviations, see Figure 3A.

glycerophospholipids revealed that the total level of LPE was increased significantly as a result of increased levels of LPE18:0 and LPE18:1 (Figure 6C). The increased level of LPE and the changes in PE and PS compositions indicate marked glycerophospholipid remodeling in response to cold exposure. This is in line with our finding that cold exposure results in increased expression of several genes involved in synthesis and remodeling of PC, PE, LPE, and PS in iBAT; e.g., *Pla2g2e*, *Pla2g12a*, *Agpat 1/3*, and phosphatidylserine synthase 2 (*Ptdss2*) (Figure 7). In contrast, cold exposure did not change the total levels or molecular composition of phosphatidylinositol (PI), sphingomyelin (SM), and alkenyl-linked PE (PE-P) in iBAT of cold-exposed mice (Figure S2). Moreover, alkyl- and alkenyl-linked PC (PC-O and PC-P, respectively) and alkenyl-linked PE (PE-O) were only detected in iBAT of the control or cold-treated mice, respectively (Figure S2). Taken together, we demonstrate that cold exposure activates the transcriptional program of glycerophospholipid metabolism in iBAT and that this is accompanied by remodeling of the glycerophospholipid composition in a highly subspecies-specific manner as early as 3 days following cold exposure.

DISCUSSION

The expansion of BAT thermogenic capacity by cold exposure is a multistep process that entails a complex interplay between transcriptional and metabolic signaling pathways. In this study, we applied RNA-seq and mass-spectrometry-based lipidomics with the aim of providing a resource that describes the molecular signature at the level of the transcriptome and lipidome for the activation of mouse iBAT during short-term (3-day) cold challenge (4°C). Furthermore, we compared global profiling by RNA-seq with that of previous studies to help identify genes that mediate cold-induced recruitment of thermogenically active BAT.

Our integrated results indicate that cold challenge induces gene programs involved in glycerolipid and glycerophospholipid metabolism as well as fatty acid elongation. This is accompanied by a highly selective increase in the abundance of long- and very-long- as well as odd-chain acyls in TAG and highly subspecies-selective changes of acyl chain compositions in glycerophospholipids.

Unlike some previous studies (Hao et al., 2015; Rosell et al., 2014), we did not observe increased expression of genes involved in oxidative phosphorylation and glycolysis. We consider it possible that this is due to the fact that mice in these particular previous studies were housed at thermoneutrality and subsequently exposed to cold, whereas mice in our study (and other studies that did not demonstrate this effect) were housed at room temperature prior to cold exposure. Therefore,

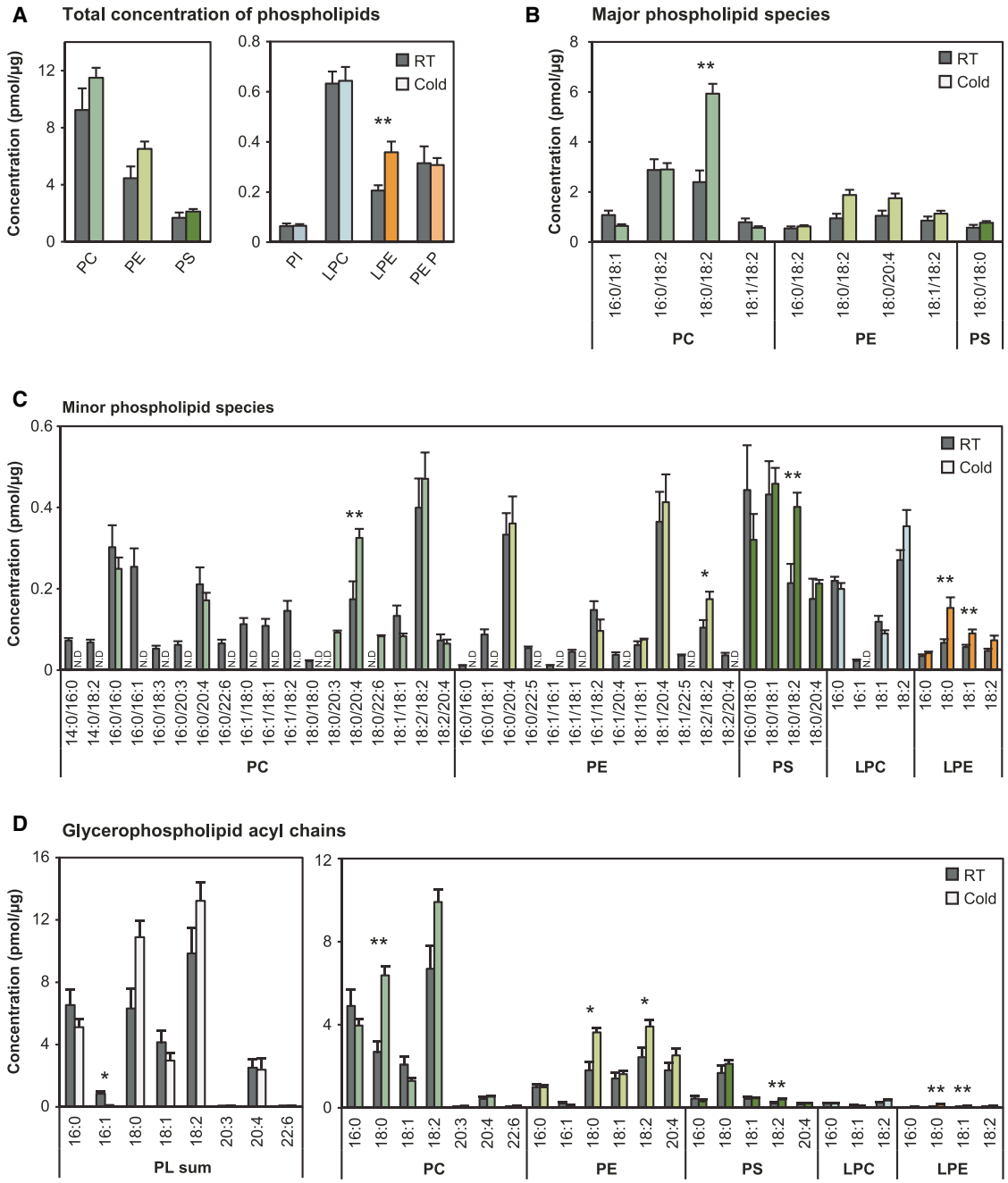

Figure 6. Cold-Mediated Changes in Glycerophospholipid Composition and Fatty Acyl Levels in iBAT

Lipidomics analysis of iBAT from mice kept at room temperature or exposed to cold (4°C) for 3 days. Lipids were extracted and analyzed as described in the Experimental Procedures.

(A) The concentration of the quantified glycerophospholipid classes in iBAT from cold-treated and control mice. Data are presented as means + SEM; n = 3–5 for both groups. Significance level: **p < 0.01.

(B and C) The concentration of the quantified glycerophospholipid species in iBAT from cold-treated and control mice. Data are presented as means + SEM; n = 3–5 for both groups. Significance levels: *p < 0.05, **p < 0.01. The species are divided into major (B) and minor (C) species based on abundance.

(D) The concentration of the individual acyl chains associated with glycerophospholipids in iBAT of cold-treated (n = 5) and control (n = 4–5) mice. The PL sum is the sum of the concentrations of the quantified fatty acyls from all glycerophospholipid classes. Data are presented as means + SEM. *p < 0.05, **p < 0.01. See also Figure S2.

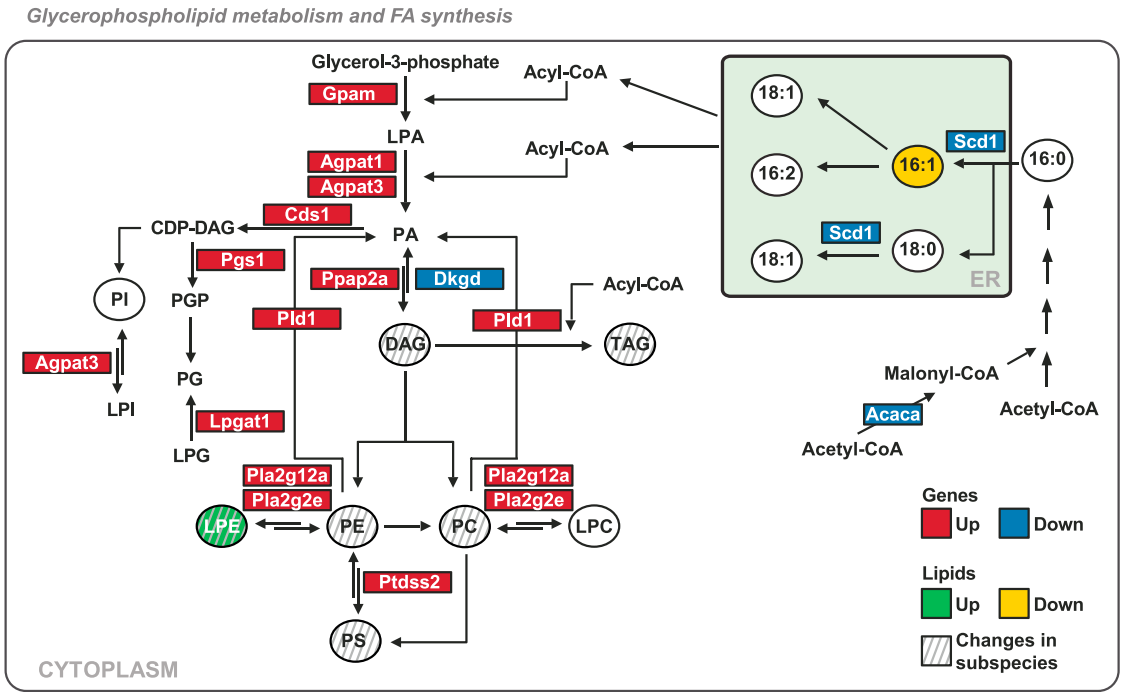

Figure 7. The Glycerophospholipid Pathway Is Induced in iBAT upon Cold Exposure

Selected glycerophospholipid and fatty acid elongation metabolic reactions from KEGG, with indications of quantified lipid classes or acyl chains in glycerophospholipids (circles) and genes (rectangles) regulated significantly in iBAT by short-term cold exposure. Colors indicate increased (red) or decreased (blue) expression levels of genes (encoding proteins that catalyze the indicated conversions) upon cold exposure or increased (green), decreased (yellow), or unchanged (white) levels of the total concentration of the lipid classes. Lipid classes in which individual subspecies are altered by cold exposure are hatched. LPA, lysophosphatidic acid; LPG, lysophosphatidylglycerol; PG, phosphatidylglycerol; PGP, phosphatidylglycerophosphate; LPI, lysophosphatidylinositol; *Cds1*, CDP-diacylglycerol synthase 1; *Pgs1*, phosphatidylglycerophosphate synthase 1; *Pld1*, phospholipase D1; *Lpgat1*, lysophosphatidylglycerol acyltransferase 1. For other abbreviations, see Figure 3A.

this raises the interesting possibility that activation of glycolysis and oxidative phosphorylation represents a first defense against the cold challenge, when the temperature is reduced from thermoneutrality, whereas the lipid remodeling represents a second defense that is primarily activated when the temperature is reduced further and that facilitates the adaptation of brown adipocytes to the increased need for respiratory capacity.

One of the several interesting findings from our study is that short-term cold exposure of mice dramatically upregulated mRNA levels of *Fndc5* (>8-fold), the gene encoding the prohormone FNDC5, which is processed and released into the bloodstream as the hormone irisin. Irisin has been reported previously to be an exercise-induced myokine that drives brown fat-like thermogenesis in murine white fat (Boström et al., 2012). Furthermore, serum irisin levels have been shown recently to rise in a shivering-dependent manner in humans exposed to cold (Lee et al., 2014). Although *Fndc5* is expressed to much lower levels in adipocytes compared with muscle cells (Huh et al., 2012), subcutaneous WAT secretes significant levels of irisin, which is elevated during exercise (Roca-Rivada et al., 2013). Our data raise the possibility that the remarkable cold-induced upregulation of *Fndc5* expression in BAT increases local concentrations of irisin, which, in a paracrine manner, could contribute to the thermogenic action in fat tissues. We also identified the transcriptional regulator *KLF11* as a cold-inducible gene in murine BAT. We recently reported that KLF11 is required for rosiglitazone-induced browning of human white adipocytes and that expression of this factor in human browned adipocytes is elevated by thermogenic stimuli (Loft et al., 2015). Others have shown that KLF11 is induced in subcutaneous WAT of mice after 10 days of cold exposure (Rosell et al., 2014). The results of our study indicate that KLF11 may also be involved in the cold response in BAT. The biological and physiological importance of the marked cold-induced upregulation of *Fndc5* and *Klf11* should be investigated further using in vivo adipocyte-specific knockout models.

It has been reported previously that expression of specific genes involved in fatty acid elongation; e.g., *Elovl3* (Jakobsson et al., 2006), and in glycerophospholipid metabolism, e.g., *Pla2g2e* and several *Agpat*s (Hao et al., 2015; Rosell et al., 2014), is induced in response to cold exposure. However, our study indicates that expression of a large number of genes in these pathways is induced significantly in iBAT in response to a cold challenge. Interestingly, enzymes from the glycerophospholipid pathways that are associated with the mitochondrial membrane have been shown recently to be upregulated in the mitochondrial proteome of iBAT in mice exposed to cold for 4 days (Forner et al., 2009), thereby indicating that the transcriptional changes in this pathway are accompanied by changes at the protein/enzyme level. Furthermore, we found that cold leads

to increased *Acsl5* mRNA levels, which is consistent with previous findings showing that cold exposure increased the mitochondrial levels of ACSL5 protein 5-fold (Forner et al., 2009). It is possible that ACSL5 plays an important role in TAG remodeling because it specifically facilitates re-acylation of TAG in rat hepatoma cells (Mashek et al., 2006).

Based on the effects of short-term cold exposure on the transcriptome, we chose to focus our analyses of the lipidome on TAG and glycerophospholipids. Using mass spectrometry, we identified cold-induced changes in the composition of specific lipid classes and demonstrated lipid class-specific remodeling of the acyl chain composition.

Of the major lipid classes analyzed, only the concentration of CE was altered significantly. The increase in CE in iBAT in response to cold most likely reflects an increased uptake of lipoproteins from the circulation. It has been demonstrated recently that iBAT has a high capacity for glucose disposal and TAG clearance from the circulation and that this is increased in response to cold (Bartelt et al., 2011; Labbe et al., 2015). TAG clearance occurs primarily following extracellular lipolysis and leaves the CE-rich remnants for clearance, mostly by the liver. However, cold exposure also leads to an increased uptake of labeled cholesteryl ester in iBAT (Berbée et al., 2015; Khedoe et al., 2015).

Short-term cold exposure led to enrichment of TAG with long and very long acyl chains in iBAT, most notably of the C18:0, C20:0, and C22:0 acyl chains. Intriguingly, C18:0 has been shown recently to be a signaling molecule important for increased mitochondrial biogenesis and function in *Drosophila* and human cell lines (Senyilmaz et al., 2015). This raises the interesting possibility that the accumulation of C18:0 in iBAT upon short-term cold exposure is involved in the cellular adaptation; e.g., increased respiratory capacity. Furthermore, we demonstrate that cold exposure increases the level of odd-numbered acyl chains in TAG. Because of their low abundance, odd-chain fatty acids have been used previously as internal standards in gas-liquid chromatography analysis (Jenkins et al., 2015), which might have masked the detection of endogenous levels. We propose that a small number of the long and very long acyl chains accumulate in iBAT upon short-term cold exposure and might be channeled toward the α-oxidation pathway in the peroxisomes, which is normally used for oxidation of branched-chain fatty acids. Odd-chain fatty acids generated in this way can enter the classical β-oxidation pathway. In keeping with this, it has been shown recently that differentiating 3T3-L1 and primary adipocytes are able to produce odd-chain fatty acids and that the levels of TAG and other lipid species containing these fatty acids increase during the differentiation of the adipocytes (Roberts et al., 2009; Su et al., 2004). Interestingly, peroxisomal α- and β-oxidation of fatty acids are uncoupled from ATP production, meaning that energy from these reactions is released as heat (Nedergaard et al., 1980). Future investigations should determine whether peroxisomal α- and β-oxidation of long-chain fatty acids are enhanced by cold exposure and determine the extent to which this contributes to heat production in BAT.

We also observed a significant remodeling of glycerophospholipids in response to cold. It has been reported previously that long-term (>1 week) cold exposure causes a significant remodeling of the composition of acyl chains in the total pool of mitochondrial phospholipids in BAT (Ocloo et al., 2007, and references therein) through adrenergic stimulation via the sympathetic nervous system (Mory et al., 1988; Mory et al., 1980). Similar to previous long-term studies (Ocloo et al., 2007; Ricquier et al., 1979), we observed a dramatic decrease in C16:1 in glycerophospholipids in response to short-term cold exposure, and our lipidomics approach allowed us to demonstrate that this is associated with reduced abundance of PC, PE, and LPC species containing C16:1. It is possible that the cold-induced decrease in C16:1 is caused by the decrease in *Scd1* expression, the main gene responsible for desaturation of palmitic and stearic acid. Interestingly, the cold-induced decrease in C16:1 is only detected for selected glycerophospholipids and not in TAG.

Our data demonstrate that TAG and glycerophospholipids are not only modulated differentially, but phospholipid subspecies are also remodeled selectively by cold exposure. Importantly, this indicates that cold-induced remodeling of glycerolipids is not primarily driven by general effects on fatty acid metabolism or by increased food intake but, rather, the result of a complex regulation of glycerolipid metabolism. The mechanistic basis for this subspecies-selective remodeling of glycerolipids is unknown. However, it is possible that it reflects the differential effect of cold on substrate availability or affinities of enzymes involved in glycerophospholipid and TAG synthesis and remodeling. Such enzymes include membrane-bound O-acyltransferases and DGATs (Yamashita et al., 2014). Alternatively, cold may induce differential retention of acyl chains in different phospholipid subclasses and subspecies. In this regard, it has been shown that C18:0, C18:2, and C20:4 phospholipid acyl chains increase during fasting, possibly because of low mobilization that leads to a relative retention of these acyl chains in BAT phospholipids (Groscolas and Herzberg, 1997). The highly selective remodeling of glycerophospholipid subspecies is likely to have significant functional implications during cold adaptation. Glycerophospholipids act as ligands for ligand-activated transcription factors, e.g., PPARγ (Lodhi et al., 2012), and the cold-mediated shift in the pool of available glycerophospholipid subspecies may affect signaling cascades and transcription factors driving the cold-induced thermogenic gene program. Future studies should focus on examining the contributions of specific glycerophospholipid subspecies in mediating the thermogenic response in BAT and their importance for activating ligand-dependent transcriptions factors.

In summary, we determined the cold-induced adaptive changes in the transcriptome and lipidome of iBAT using advanced omics techniques. Our data therefore constitute a comprehensive and valuable resource that stimulates new hypotheses regarding the functional importance of cold-induced changes in the BAT transcriptome and lipidome. One key finding is that cold adaptation entails a markedly increased expression of genes involved in glycerolipid synthesis and fatty acid elongation that is accompanied by remodeling of glycerophospholipids and TAG in a manner that is highly subspecies-selective. Future studies are required to determine the functional consequences of this remodeling of glycerolipids in iBAT.

EXPERIMENTAL PROCEDURES

Additional methods are available in the Supplemental Experimental Procedures.

Animals

Male C57BL6/JBomTac mice were single-housed under standard laboratory conditions, including a 12-hr light/dark cycle, with free access to chow and water. Five mice were housed at either 22°C ± 3°C or at 4°C for 3 days and subsequently killed by cervical dislocation. iBAT was dissected, frozen immediately in liquid nitrogen, and stored at −80°C. To minimize individual variation, the mice were fasted for 2 hr before termination. All animal breeding and experimentation were approved by the Danish Animal Experiment Inspectorate.

Isolation of RNA and RNA-Seq Preparation

iBAT was homogenized in Isol-RNA lysis reagent (5 Prime) and purified with the Total RNA purification kit (Norgen Biotek) according to the manufacturers' protocols. The integrity of the RNA was confirmed using a Bioanalyzer 2100 (Agilent Technologies). 4 μg of column-purified total RNA from iBAT was polyA-selected and subsequently subjected to fragmentation and cDNA synthesis using the TruSeq RNA sample prep kit v2 (Illumina). RNA-seq libraries were constructed according to the manufacturer's instructions (Illumina) as described previously (Nielsen and Mandrup, 2014) and sequenced using the Illumina HiSeq 1500 platform.

RNA-Seq Data Analysis

The sequenced 50-base pair single-end reads were quality-checked using FastQC and subsequently aligned to the mouse reference genome (version mm9) using STAR (Dobin et al., 2013) with default parameters. The number of exon reads for all RefSeq genes were counted using iRNA-seq (Madsen et al., 2015), only keeping the longest RefSeq transcripts for further analyses. The resulting count matrix was analyzed with EdgeR (Robinson et al., 2010), and HTSFilter was applied to filter out genes with low, constant levels of expression under the two conditions (Rau et al., 2013). Differential expression was determined using a cutoff significance level of FDR < 0.05. Functional enrichment analysis was performed with HOMER (Heinz et al., 2010) using pathways related to metabolism from the KEGG database annotation (Kanehisa and Goto, 2000; Kanehisa et al., 2014).

Additional Datasets

Transcriptomics data from previous studies were obtained from GEO and analyzed. Data obtained by DGE profiling (GSE63031, Hao et al., 2015) were analyzed using EdgeR and HTSFilter as described above. Microarray-based data (GSE51080, Rosell et al., 2014; GSE44138, Shore et al., 2013; and GSE40486, Plaisier et al., 2012) were extracted from GEO using the GEO2R online tool (Barrett et al., 2013). See the Supplemental Experimental Procedures for more details.

Lipid Sample Preparation and Lipidomics Analyses

Lipid extraction, mass-spectrometry-based lipid detection, and data analysis were performed by Zora Biosciences (Jung et al., 2011). In shotgun and triacylglycerol lipidomics, lipid extracts were analyzed on a hybrid triple quadrupole/linear ion trap mass spectrometer (QTRAP 5500) equipped with a robotic nanoflow ion source (NanoMate HD) as described previously (Ståhlman et al., 2009). Molecular lipids were analyzed in both positive and negative ion modes using multiple precursor ion scanning-based methods (Ekroos et al., 2002, 2003). The molecular lipid species were identified and quantified in absolute (TAG, CE, PC, PE, PS, LPC, LPE, diacylglycerol [DAG], and SM) or semi-absolute (PI, PC-O, PC-P, PE-O, and PE-P) amounts (Ejsing et al., 2006) and normalized to their respective internal standard and the sample amount. The concentrations of molecular lipids are presented as picomoles per microgram wet tissue weight. The lipids are referred to according to the LIPID MAPS lipid nomenclature recommendations (Fahy et al., 2009; Liebisch et al., 2013). A rank-sum Wilcoxon statistical analysis was performed to compare the lipid concentrations of the groups. Because of the limited number of samples, exact p values were computed using Monte Carlo estimation. $p < 0.05$ was considered significant. The relative difference (percent) between the two groups was estimated using the Hodges-Lehmann estimator. A complete list of the lipidomics data is provided in Table S4.

ACCESSION NUMBERS

The accession number for the sequencing data reported in this paper is GEO: GSE70437.

SUPPLEMENTAL INFORMATION

Supplemental Information includes Supplemental Experimental Procedures, two figures, and four tables and can be found with this article online at http://dx.doi.org/10.1016/j.celrep.2015.10.069.

AUTHOR CONTRIBUTIONS

A.B.M. and S.M. conceived and designed the study. A.B.M. performed the mouse experiments. R.N. performed the sequencing experiments. T.V. and K.E. (Zora Biosciences) performed the lipidomics experiments. A.L. analyzed the transcriptomics data with input from J.G.S.M. T.V., K.E., M.S.A., and A.B.M. analyzed the lipidomics data. A.B.M., A.L., and S.M. interpreted the results of experiments, prepared figures, and wrote the manuscript. All authors approved the final version of the manuscript.

ACKNOWLEDGMENTS

The authors thank members of the S.M. lab for experimental guidance and discussions and J. Granneman and N. Færgeman for valuable inputs to the manuscript. This work was supported by The Danish Independent Research Council/Natural Science, the Novo Nordisk Foundation, the Lundbeck Foundation, the VILLUM Foundation through a grant to the VILLUM Center for Bioanalytical Sciences at the University of Southern Denmark, and NordForsk through a grant to the Nordic Center of Excellence MitoHealth.

Received: July 17, 2015
Revised: September 15, 2015
Accepted: October 22, 2015
Published: November 25, 2015

REFERENCES

Barrett, T., Wilhite, S.E., Ledoux, P., Evangelista, C., Kim, I.F., Tomashevsky, M., Marshall, K.A., Phillippy, K.H., Sherman, P.M., Holko, M., et al. (2013). NCBI GEO: archive for functional genomics data sets–update. Nucleic Acids Res. *41*, D991–D995.

Bartelt, A., Bruns, O.T., Reimer, R., Hohenberg, H., Ittrich, H., Peldschus, K., Kaul, M.G., Tromsdorf, U.I., Weller, H., Waurisch, C., et al. (2011). Brown adipose tissue activity controls triglyceride clearance. Nat. Med. *17*, 200–205.

Berbée, J.F., Boon, M.R., Khedoe, P.P., Bartelt, A., Schlein, C., Worthmann, A., Kooijman, S., Hoeke, G., Mol, I.M., John, C., et al. (2015). Brown fat activation reduces hypercholesterolaemia and protects from atherosclerosis development. Nat. Commun. *6*, 6356.

Boström, P., Wu, J., Jedrychowski, M.P., Korde, A., Ye, L., Lo, J.C., Rasbach, K.A., Boström, E.A., Choi, J.H., Long, J.Z., et al. (2012). A PGC1-α-dependent myokine that drives brown-fat-like development of white fat and thermogenesis. Nature *481*, 463–468.

Cannon, B., and Nedergaard, J. (2004). Brown adipose tissue: function and physiological significance. Physiol. Rev. *84*, 277–359.

Chartoumpekis, D.V., Habeos, I.G., Ziros, P.G., Psyrogiannis, A.I., Kyriazopoulou, V.E., and Papavassiliou, A.G. (2011). Brown adipose tissue responds to cold and adrenergic stimulation by induction of FGF21. Mol. Med. *17*, 736–740.

Cinti, S. (2005). The adipose organ. Prostaglandins Leukot. Essent. Fatty Acids *73*, 9–15.

Dobin, A., Davis, C.A., Schlesinger, F., Drenkow, J., Zaleski, C., Jha, S., Batut, P., Chaisson, M., and Gingeras, T.R. (2013). STAR: ultrafast universal RNA-seq aligner. Bioinformatics *29*, 15–21.

Ejsing, C.S., Duchoslav, E., Sampaio, J., Simons, K., Bonner, R., Thiele, C., Ekroos, K., and Shevchenko, A. (2006). Automated identification and quantification of glycerophospholipid molecular species by multiple precursor ion scanning. Anal. Chem. *78*, 6202–6214.

Ekroos, K., Chernushevich, I.V., Simons, K., and Shevchenko, A. (2002). Quantitative profiling of phospholipids by multiple precursor ion scanning on a hybrid quadrupole time-of-flight mass spectrometer. Anal. Chem. *74*, 941–949.

Ekroos, K., Ejsing, C.S., Bahr, U., Karas, M., Simons, K., and Shevchenko, A. (2003). Charting molecular composition of phosphatidylcholines by fatty acid scanning and ion trap MS3 fragmentation. J. Lipid Res. *44*, 2181–2192.

Fahy, E., Subramaniam, S., Murphy, R.C., Nishijima, M., Raetz, C.R., Shimizu, T., Spener, F., van Meer, G., Wakelam, M.J., and Dennis, E.A. (2009). Update of the LIPID MAPS comprehensive classification system for lipids. J. Lipid Res. *50* (*Suppl*), S9–S14.

Forner, F., Kumar, C., Luber, C.A., Fromme, T., Klingenspor, M., and Mann, M. (2009). Proteome differences between brown and white fat mitochondria reveal specialized metabolic functions. Cell Metab. *10*, 324–335.

Fujino, T., Asaba, H., Kang, M.J., Ikeda, Y., Sone, H., Takada, S., Kim, D.H., Ioka, R.X., Ono, M., Tomoyori, H., et al. (2003). Low-density lipoprotein receptor-related protein 5 (LRP5) is essential for normal cholesterol metabolism and glucose-induced insulin secretion. Proc. Natl. Acad. Sci. USA *100*, 229–234.

Golozoubova, V., Gullberg, H., Matthias, A., Cannon, B., Vennström, B., and Nedergaard, J. (2004). Depressed thermogenesis but competent brown adipose tissue recruitment in mice devoid of all hormone-binding thyroid hormone receptors. Mol. Endocrinol. *18*, 384–401.

Grefhorst, A., van den Beukel, J.C., van Houten, E.L., Steenbergen, J., Visser, J.A., and Themmen, A.P. (2015). Estrogens increase expression of bone morphogenetic protein 8b in brown adipose tissue of mice. Biol. Sex Differ. *6*, 7.

Groscolas, R., and Herzberg, G.R. (1997). Fasting-induced selective mobilization of brown adipose tissue fatty acids. J. Lipid Res. *38*, 228–238.

Guillou, H., Zadravec, D., Martin, P.G., and Jacobsson, A. (2010). The key roles of elongases and desaturases in mammalian fatty acid metabolism: Insights from transgenic mice. Prog. Lipid Res. *49*, 186–199.

Hao, Q., Yadav, R., Basse, A.L., Petersen, S., Sonne, S.B., Rasmussen, S., Zhu, Q., Lu, Z., Wang, J., Audouze, K., et al. (2015). Transcriptome profiling of brown adipose tissue during cold exposure reveals extensive regulation of glucose metabolism. Am. J. Physiol. Endocrinol. Metab. *308*, E380–E392.

Harada-Shiba, M., Takagi, A., Marutsuka, K., Moriguchi, S., Yagyu, H., Ishibashi, S., Asada, Y., and Yokoyama, S. (2004). Disruption of autosomal recessive hypercholesterolemia gene shows different phenotype in vitro and in vivo. Circ. Res. *95*, 945–952.

Heinz, S., Benner, C., Spann, N., Bertolino, E., Lin, Y.C., Laslo, P., Cheng, J.X., Murre, C., Singh, H., and Glass, C.K. (2010). Simple combinations of lineage-determining transcription factors prime cis-regulatory elements required for macrophage and B cell identities. Mol. Cell *38*, 576–589.

Hondares, E., Iglesias, R., Giralt, A., Gonzalez, F.J., Giralt, M., Mampel, T., and Villarroya, F. (2011). Thermogenic activation induces FGF21 expression and release in brown adipose tissue. J. Biol. Chem. *286*, 12983–12990.

Huh, J.Y., Panagiotou, G., Mougios, V., Brinkoetter, M., Vamvini, M.T., Schneider, B.E., and Mantzoros, C.S. (2012). FNDC5 and irisin in humans: I. Predictors of circulating concentrations in serum and plasma and II. mRNA expression and circulating concentrations in response to weight loss and exercise. Metabolism *61*, 1725–1738.

Jakobsson, A., Westerberg, R., and Jacobsson, A. (2006). Fatty acid elongases in mammals: their regulation and roles in metabolism. Prog. Lipid Res. *45*, 237–249.

Jenkins, B., West, J.A., and Koulman, A. (2015). A review of odd-chain fatty acid metabolism and the role of pentadecanoic Acid (c15:0) and heptadecanoic Acid (c17:0) in health and disease. Molecules *20*, 2425–2444.

Jung, H.R., Sylvänne, T., Koistinen, K.M., Tarasov, K., Kauhanen, D., and Ekroos, K. (2011). High throughput quantitative molecular lipidomics. Biochim. Biophys. Acta *1811*, 925–934.

Kanehisa, M., and Goto, S. (2000). KEGG: Kyoto Encyclopedia of Genes and Genomes. Nucleic Acids Res. *28*, 27–30.

Kanehisa, M., Goto, S., Sato, Y., Kawashima, M., Furumichi, M., and Tanabe, M. (2014). Data, information, knowledge and principle: back to metabolism in KEGG. Nucleic Acids Res. *42*, D199–D205.

Khedoe, P.P., Hoeke, G., Kooijman, S., Dijk, W., Buijs, J.T., Kersten, S., Havekes, L.M., Hiemstra, P.S., Berbée, J.F., Boon, M.R., and Rensen, P.C. (2015). Brown adipose tissue takes up plasma triglycerides mostly after lipolysis. J. Lipid Res. *56*, 51–59.

Labbe, S.M., Caron, A., Bakan, I., Laplante, M., Carpentier, A.C., Lecomte, R., and Richard, D. (2015). In vivo measurement of energy substrate contribution to cold-induced brown adipose tissue thermogenesis. FASEB J. *29*, 2046–2058.

Lee, P., Linderman, J.D., Smith, S., Brychta, R.J., Wang, J., Idelson, C., Perron, R.M., Werner, C.D., Phan, G.Q., Kammula, U.S., et al. (2014). Irisin and FGF21 are cold-induced endocrine activators of brown fat function in humans. Cell Metab. *19*, 302–309.

Liebisch, G., Vizcaíno, J.A., Köfeler, H., Trötzmüller, M., Griffiths, W.J., Schmitz, G., Spener, F., and Wakelam, M.J. (2013). Shorthand notation for lipid structures derived from mass spectrometry. J. Lipid Res. *54*, 1523–1530.

Lodhi, I.J., Yin, L., Jensen-Urstad, A.P., Funai, K., Coleman, T., Baird, J.H., El Ramahi, M.K., Razani, B., Song, H., Fu-Hsu, F., et al. (2012). Inhibiting adipose tissue lipogenesis reprograms thermogenesis and PPARγ activation to decrease diet-induced obesity. Cell Metab. *16*, 189–201.

Loft, A., Forss, I., Siersbæk, M.S., Schmidt, S.F., Larsen, A.S., Madsen, J.G., Pisani, D.F., Nielsen, R., Aagaard, M.M., Mathison, A., et al. (2015). Browning of human adipocytes requires KLF11 and reprogramming of PPARγ superenhancers. Genes Dev. *29*, 7–22.

Madsen, J.G., Schmidt, S.F., Larsen, B.D., Loft, A., Nielsen, R., and Mandrup, S. (2015). iRNA-seq: computational method for genome-wide assessment of acute transcriptional regulation from total RNA-seq data. Nucleic Acids Res. *43*, e40.

Mashek, D.G., McKenzie, M.A., Van Horn, C.G., and Coleman, R.A. (2006). Rat long chain acyl-CoA synthetase 5 increases fatty acid uptake and partitioning to cellular triacylglycerol in McArdle-RH7777 cells. J. Biol. Chem. *281*, 945–950.

Mory, G., Ricquier, D., and Hémon, P. (1980). Effects of chronic treatments upon the brown adipose tissue of rats. II. Comparison between the effects of catecholamine injections and cold adaptation. J. Physiol. (Paris) *76*, 859–864.

Mory, G., Gawer, M., and Kader, J.C. (1988). Effect of noradrenaline chronic administration on brown fat phospholipids. Biosci. Rep. *8*, 465–469.

Nedergaard, J., Alexson, S., and Cannon, B. (1980). Cold adaptation in the rat: increased brown fat peroxisomal beta-oxidation relative to maximal mitochondrial oxidative capacity. Am. J. Physiol. *239*, C208–C216.

Nielsen, R., and Mandrup, S. (2014). Genome-wide profiling of transcription factor binding and epigenetic marks in adipocytes by ChIP-seq. Methods Enzymol. *537*, 261–279.

Ocloo, A., Shabalina, I.G., Nedergaard, J., and Brand, M.D. (2007). Cold-induced alterations of phospholipid fatty acyl composition in brown adipose tissue mitochondria are independent of uncoupling protein-1. Am. J. Physiol. Regul. Integr. Comp. Physiol. *293*, R1086–R1093.

Petrović, V., Buzadzić, B., Korać, A., Vasilijević, A., Janković, A., and Korać, B. (2006). Free radical equilibrium in interscapular brown adipose tissue: relationship between metabolic profile and antioxidative defense. Comp. Biochem. Physiol. C Toxicol. Pharmacol. *142*, 60–65.

Plaisier, C.L., Bennett, B.J., He, A., Guan, B., Lusis, A.J., Reue, K., and Vergnes, L. (2012). Zbtb16 has a role in brown adipocyte bioenergetics. Nutr. Diabetes *2*, e46.

Rau, A., Gallopin, M., Celeux, G., and Jaffrézic, F. (2013). Data-based filtering for replicated high-throughput transcriptome sequencing experiments. Bioinformatics *29*, 2146–2152.

Ricquier, D., Mory, G., and Hemon, P. (1979). Changes induced by cold adaptation in the brown adipose tissue from several species of rodents, with special reference to the mitochondrial components. Can. J. Biochem. *57*, 1262–1266.

Roberts, L.D., Virtue, S., Vidal-Puig, A., Nicholls, A.W., and Griffin, J.L. (2009). Metabolic phenotyping of a model of adipocyte differentiation. Physiol. Genomics *39*, 109–119.

Robinson, M.D., McCarthy, D.J., and Smyth, G.K. (2010). edgeR: a Bioconductor package for differential expression analysis of digital gene expression data. Bioinformatics *26*, 139–140.

Roca-Rivada, A., Castelao, C., Senin, L.L., Landrove, M.O., Baltar, J., Belén Crujeiras, A., Seoane, L.M., Casanueva, F.F., and Pardo, M. (2013). FNDC5/irisin is not only a myokine but also an adipokine. PLoS ONE *8*, e60563.

Roncari, D.A., and Mack, E.Y. (1976). Mammalian fatty acid synthetase. III. Characterization of human liver synthetase products and kinetics of methylmalonyl-CoA inhibition. Can. J. Biochem. *54*, 923–926.

Rosell, M., Kaforou, M., Frontini, A., Okolo, A., Chan, Y.W., Nikolopoulou, E., Millership, S., Fenech, M.E., MacIntyre, D., Turner, J.O., et al. (2014). Brown and white adipose tissues: intrinsic differences in gene expression and response to cold exposure in mice. Am. J. Physiol. Endocrinol. Metab. *306*, E945–E964.

Senyilmaz, D., Virtue, S., Xu, X., Tan, C.Y., Griffin, J.L., Miller, A.K., Vidal-Puig, A., and Teleman, A.A. (2015). Regulation of mitochondrial morphology and function by stearoylation of TFR1. Nature *525*, 124–128.

Seyama, Y., Otsuka, H., Kawaguchi, A., and Yamakawa, T. (1981). Fatty acid synthetase from the Harderian gland of guinea pig: biosynthesis of methyl-branched fatty acids. J. Biochem. *90*, 789–797.

Shore, A.M., Karamitri, A., Kemp, P., Speakman, J.R., Graham, N.S., and Lomax, M.A. (2013). Cold-induced changes in gene expression in brown adipose tissue, white adipose tissue and liver. PLoS ONE *8*, e68933.

Smith, S. (1994). The animal fatty acid synthase: one gene, one polypeptide, seven enzymes. FASEB J. *8*, 1248–1259.

Ståhlman, M., Ejsing, C.S., Tarasov, K., Perman, J., Borén, J., and Ekroos, K. (2009). High-throughput shotgun lipidomics by quadrupole time-of-flight mass spectrometry. J. Chromatogr. B Analyt. Technol. Biomed. Life Sci. *877*, 2664–2672.

Su, X., Han, X., Yang, J., Mancuso, D.J., Chen, J., Bickel, P.E., and Gross, R.W. (2004). Sequential ordered fatty acid alpha oxidation and Delta9 desaturation are major determinants of lipid storage and utilization in differentiating adipocytes. Biochemistry *43*, 5033–5044.

Waldén, T.B., Hansen, I.R., Timmons, J.A., Cannon, B., and Nedergaard, J. (2012). Recruited vs. nonrecruited molecular signatures of brown, "brite," and white adipose tissues. Am. J. Physiol. Endocrinol. Metab. *302*, E19–E31.

Westerberg, R., Månsson, J.E., Golozoubova, V., Shabalina, I.G., Backlund, E.C., Tvrdik, P., Retterstøl, K., Capecchi, M.R., and Jacobsson, A. (2006). ELOVL3 is an important component for early onset of lipid recruitment in brown adipose tissue. J. Biol. Chem. *281*, 4958–4968.

Whittle, A.J., Carobbio, S., Martins, L., Slawik, M., Hondares, E., Vázquez, M.J., Morgan, D., Csikasz, R.I., Gallego, R., Rodriguez-Cuenca, S., et al. (2012). BMP8B increases brown adipose tissue thermogenesis through both central and peripheral actions. Cell *149*, 871–885.

Xue, Y., Petrovic, N., Cao, R., Larsson, O., Lim, S., Chen, S., Feldmann, H.M., Liang, Z., Zhu, Z., Nedergaard, J., et al. (2009). Hypoxia-independent angiogenesis in adipose tissues during cold acclimation. Cell Metab. *9*, 99–109.

Yamashita, A., Hayashi, Y., Nemoto-Sasaki, Y., Ito, M., Oka, S., Tanikawa, T., Waku, K., and Sugiura, T. (2014). Acyltransferases and transacylases that determine the fatty acid composition of glycerolipids and the metabolism of bioactive lipid mediators in mammalian cells and model organisms. Prog. Lipid Res. *53*, 18–81.

Yu, X.X., Lewin, D.A., Forrest, W., and Adams, S.H. (2002). Cold elicits the simultaneous induction of fatty acid synthesis and beta-oxidation in murine brown adipose tissue: prediction from differential gene expression and confirmation in vivo. FASEB J. *16*, 155–168.